Forschung im Ingenieurwesen (2025)89:17
https://doi.org/10.1007/s10010-025-00784-4

ORIGINALARBEITEN/ORIGINALS

Detection of particle contamination and lubrication outage in journal bearings in wind turbine gearboxes using surface acoustic wave measurements and machine learning

Thomas Decker[1] · Georg Jacobs[1] · Malte Raddatz[1] · Julian Röder[1] · Jonas Betscher[1] · Philipp Arneth[2]

Received: 20 September 2024 / Accepted: 29 January 2025

Abstract

Journal bearings are used more and more in wind turbine (WT) gearboxes. Compared to rolling element bearings they are advantageous in terms of power density and reliability. Despite their reliability and theoretically unlimited fatigue life, journal bearings can be damaged by particularly critical operating conditions that do not represent normal WT operation. As journal bearing damage can occur very suddenly in the worst case, continuous monitoring of the bearing's condition is advisable. Particle contamination in the lubricant and an outage of the oil supply can be particularly harmful to the bearing. Condition monitoring systems (CMS) have the potential to detect such critical operating conditions in journal bearings before damage occurs. A detection of these conditions is crucial for preventing bearing damage and thus gearbox failure which results in turbine downtime and yield loss. If failures of journal bearings in WT gearboxes can be avoided through the use of CMS this, in the long term, has the potential to reduce maintenance and repair costs in the field application.

In this work the novel surface acoustic wave (SAW) measurement method is presented for the detection of particle contamination and lubrication outage. The SAW method is advantageous compared to conventional monitoring methods such as vibration measurements, as it is based on measuring the propagation behavior of actively introduced SAW into the bearing. This makes the method particularly robust against disturbing noise. For the evaluation of the signals and the detection of the aforementioned operational anomalies a machine learning approach is used. The latter is implemented such that an online monitoring can be performed with only a short latency between data input and evaluation.

The presented method was validated on a component test rig for journal bearings. For the experiments the SAW measurement was implemented into the test bearings. In the test campaign, the anomalies were actively induced and the bearing behavior observed over time. This work provides insight into the signals measured during the occurrence of operational anomalies and proves that a lubrication outage and particle contamination can be detected using SAW.

✉ Thomas Decker
thomas.decker@cwd.rwth-aachen.de

[1] Chair for Wind Power Drives, RWTH Aachen University, Campus-Boulevard 61, 52074 Aachen, Germany

[2] BestSens AG, Jean-Paul-Weg 2, 93489 Niederfüllbach, Germany

Published online: 19 February 2025

Erkennung von Partikelkontamination und Schmierungsausfall in Getriebegleitlagern von Windenergieanlagen mithilfe der Messung von akustischen Oberflächenwellen und maschinellem Lernen

Zusammenfassung

Gleitlager finden zunehmend in Getrieben von Windenergieanlagen (WEA) Anwendung. Im Vergleich zu Wälzlagern bieten sie Vorteile hinsichtlich Leistungsdichte und Zuverlässigkeit. Trotz ihrer hohen Zuverlässigkeit können Gleitlager durch kritische Betriebsbedingungen, die vom normalen Betrieb abweichen, beschädigt werden. Da Schäden an Gleitlagern oft plötzlich auftreten, ist eine kontinuierliche Überwachung des Lagers ratsam. Partikelkontamination im Schmiermittel und ein Ausfall der Ölversorgung sind besonders schädlich für das Lager. Zustandsüberwachungssysteme (CMS) können solche kritischen Betriebsbedingungen frühzeitig erkennen und helfen, Lagerschäden und damit Getriebeschäden zu verhindern. Durch den Einsatz von CMS lassen sich langfristig Wartungs- und Reparaturkosten senken.

In dieser Arbeit wird eine Messmethode mit akustischen Oberflächenwellen (Surface Acoustic Waves, SAW) zur Erkennung von Partikelkontamination und Ölversorgungs-Ausfällen vorgestellt. Die SAW-Methode bietet im Vergleich zu herkömmlichen Überwachungsmethoden wie Vibrationsmessungen Vorteile, da sie auf dem Ausbreitungsverhalten aktiv eingeführter SAW im Lager basiert. Dadurch ist die Methode robust gegenüber Störeinflüssen. Zur Auswertung der Signale und zur Erkennung von Betriebsanomalien wird ein maschinelles Lernverfahren eingesetzt, das eine Online-Überwachung mit minimaler Verzögerung zwischen Dateneingabe und Auswertung ermöglicht.

Die Methode wurde an einem Komponentenprüfstand für Gleitlager mit integrierter SAW-Messung validiert. In den Experimenten wurden die Anomalien aktiv induziert und das Lagerverhalten über einen bestimmten Zeitraum beobachtet. Diese Arbeit zeigt auf, dass ein Ausfall der Ölversorgung sowie Partikelkontamination mithilfe der SAW-Technologie erkannt werden können.

1 Introduction

Wind energy production is a cornerstone in the transition from fossil energy to renewable energy. With a share of around 30% of the overall electricity consumption in the year 2023 wind energy has already become the most important energy source in Germany [1, 2]. To further increase the energy output of the wind sector and to maintain its competitiveness the WT manufacturers are designing WTs with increasing rotor diameters and thus higher rated power output. Increasing rotor size leads to an increase in weight of the rotor and also the nacelle since it has to bear increasing loads. This causes an increased demand for lightweight design of the drivetrain, since the tower cannot bear ever growing weights. The gearbox is one of the heaviest components of a WT drive train. The diameter of the first planetary stage's ring gear massively contributes to the gearbox weight and size. The use of more compact journal bearings as planetary bearings instead of conventional rolling bearings is a recent driver of lightweight design of WT gearboxes. In addition, journal bearings have the potential to operate with an almost infinite lifetime when designed and operated correctly [3]. Though generally reliable under nominal operating conditions journal bearings are potentially prone to sudden failure (e.g. fretting) in the case of operational anomalies. Among those anomalies a shortfall of the bearing's lubrication with a resulting dry-running of the bearing and a contamination of the oil with particles acting as abrasives are especially critical [4]. Therefore, operational anomalies such as particle contamination and a lubrication outage due to pump malfunction are part of recent studies [5–8]. A condition monitoring system for journal bearings in WT gearboxes should be sensitive to these mechanisms to make root causes for bearing failure detectable. A fast detection of critical operating conditions is crucial. Only then the control system of the WT can initiate suitable countermeasures (e.g. derating of the WT).

2 State of the art

This section summarizes different CMS approaches, the importance of operational anomalies and the industrial use of SAW:

An established acoustic condition monitoring approach is the measurement of acoustic emissions (AE). AE can be categorized as high frequency structure borne sound and is emitted by tribological contact in the event of wear. König et. al. proved in 2021 that AE measurements can be used to detect anomalies and to distinguish between oil starvation and particle contamination in journal bearings using machine learning [9]. Similar results are presented by Poddar and Tandon [7, 8]. In [7] the detectability of particles passing through the load zone of a journal bearing using AE measurements was demonstrated for different particle sizes and concentrations. AE sound can be found in a wide frequency range and is characterized by a comparably low acoustic energy. Therefore, strong acoustic noise e.g. in

a gearbox can jeopardize the use of AE, which is potentially prone to acoustic disturbance [9].

Another possibility is the detection of an increase in temperature. In general, acoustic-based methods are faster than temperature-based methods. Nevertheless, temperature-based methods are often preferred due to the cheaper sensors and the low energy consumption. Baszenski et al. have developed an energy-autonomous temperature-based condition monitoring method for journal bearings as presented in [10].

A relatively new condition monitoring approach is the measurement of SAW [11]. SAWs are already in industrial use for condition monitoring of rolling bearings. Lindner et al. have shown that SAW correlate with the amount of lubricant in rolling bearings due to interaction of the SAWs with the lubrication gap [12, 13]. These interactions are due to an outcoupling of the SAWs into the lubrication gap [14]. The SAW method is based on the measurement of actively induced ultrasonic waves with a specific frequency on the bearing's sliding surface. This makes the SAW approach particularly robust against acoustic disturbance. Since the SAW measurement probes operate at a very high sampling rate (10 MHz [15]) it can also be considered robust against low frequency noise and vibration from the peripheral machinery of a wind turbine.

The ability to interact with the lubrication gap makes it possible for the SAW method to detect critical operating conditions before the occurrence of a failure. In case of the journal bearing, this leads to a propagation of acoustic waves in the fluid film between the surfaces of the shaft and the journal. Therefore, the propagation of the SAW is dependent of the height of the lubrication gap and possible mixed friction. This is especially important when it comes to condition monitoring of journal bearings in WTs because changes in the lubrication gap can be detected instantly.

The operational anomalies considered in this work can spontaneously cause strong abrasive wear which eventually leads to high temperature and strong adhesive wear. Therefore, these operational anomalies have been studied widely [5–8, 16, 17]. Although approaches on CMS for journal bearings and the detection of operational anomalies have been made, there is no established online CMS for journal bearings in WTs [18]. A general condition monitoring approach for journal bearings using SAW is described in [15]. In [15] Decker et al. show that the correlation between the SAW signals and the height of the lubrication gap, that Lindner et al. have shown in [13] for rolling bearings is also applicable to journal bearings [15]. The following work extends the approach made and focuses on the crucial ability of detecting the operational anomalies lubrication outage and particle-contaminated oil. Further, this work assesses the applicability of anomaly detection methods based on machine learning.

3 Method

In this section the method of the anomaly detection is presented. As mentioned above, SAW measurement systems are able to determine the amount of lubricant in journal bearings [13]. Decker et al. have shown that it is possible to predict the frictional state of a journal bearing using the combination of SAW and machine learning [15]. This paper extends the idea of using SAW and machine learning to contribute to the development of a condition monitoring system for journal bearings by presenting an approach to anomaly detection.

3.1 Measurement setup

The method applied in this work uses dispersive SAW (i.e. lamb waves) [19]. A schematic visualization of the SAW measurement setup is presented in Fig. 1.

The measurement system comprises two piezoelectric probes placed into radial boreholes next to the bearing's load zone (cf. Fig. 2) The first probe, acting as the sender, emits a transient excitation signal $u(t)$ consisting of a sinusoidal wavelet with a constant shape and frequency f_E (see Eq. 1).

$$u(t) = \sin(2 \cdot \pi \cdot f_E) \cdot \frac{1}{2}\left[1 - cos\left(\frac{2\pi n}{M-1}\right)\right] \quad (1)$$

The excitation wavelet (cf. Fig. 1a) is emitted into the bearing material once every measurement cycle with a cycle duration of 1.0 ms. At every cycle the receiver probe measures a response signal $x(t)$ containing the proportion of the excited waves that has propagated through the load zone of the bearing. An example for two measured signals received at two consecutive excitation cycles is depicted in Fig. 1b. Through the excitation different modes of SAW are created. Due to the fact that the SAWs are dispersive, the modes have different propagations speeds and arrive at the receiver separately in close succession. This leads to a measured response signal $x(t)$ that is presented in Fig. 1. The receiver signal is dependent on the frictional state of the journal bearing in terms of wave amplitude and speed. This can be quantified by measuring the propagation time τ and the amplitude u of one specific phase of the receiver signal $x(t)$ at every excitation cycle (the sampling frequency of the signal features τ and u is 1 kHz accordingly). The phase tracked by the system is set through the so-called gate position t_G (cf. Fig. 3).

It has been demonstrated in previous studies, that the aforementioned signal features are sensitive to the operational behavior of a hydrodynamic journal bearing [15, 20]. It was demonstrated, that the modulation width of the prop-

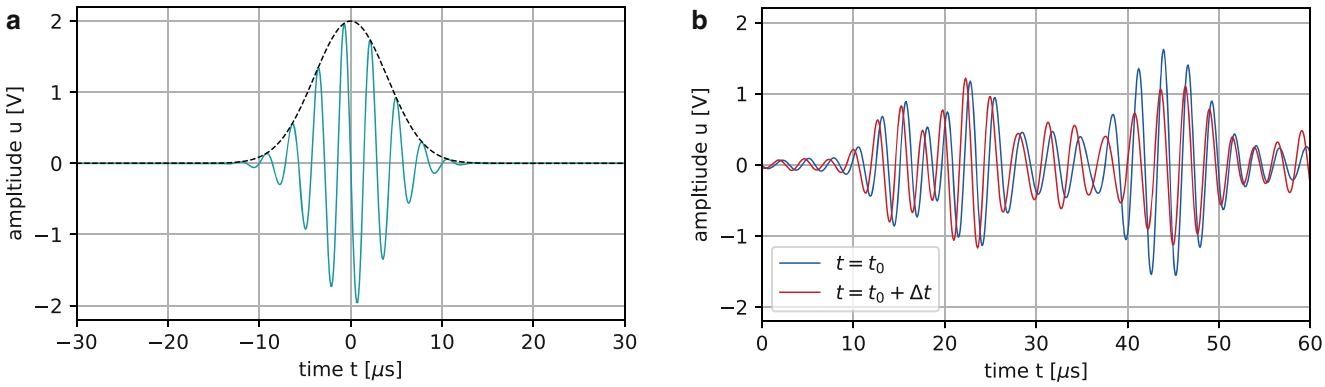

Fig. 1 Exemplary plots of a SAW excitation signal (**a**) and measured signal at two excitation cycles (**b**)

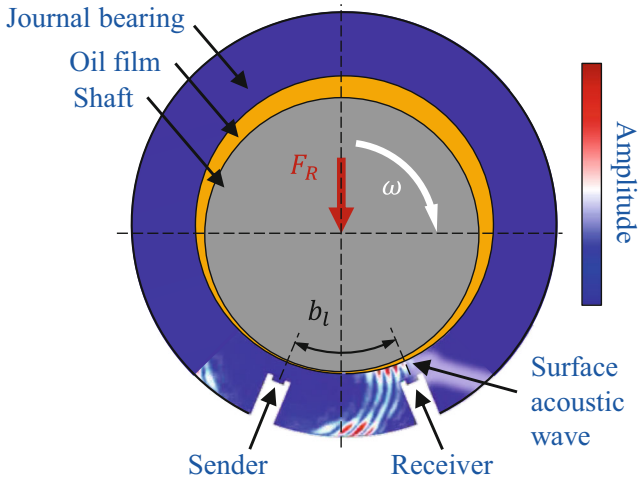

Fig. 2 Schematic visualization of the SAW measurement setup on a radial journal bearing based on [15]

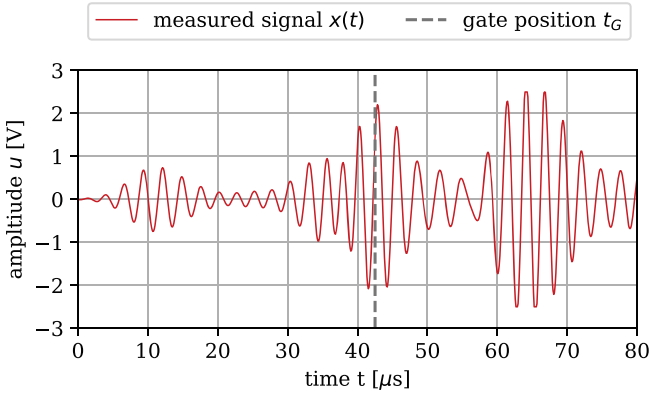

Fig. 3 Example of a measured SAW signal with the gate position marked at 42 µs

agation time signal τ in a specified time range also referred to as propagation time modulation

$$\Delta\tau = \max\left(\tau\left(t\right)\right) - \min\left(\tau\left(t\right)\right), t \in \left[t_0, t_1\right], \tag{2}$$

is especially sensitive to mixed friction events. For the context of this work it is assumed, that this finding is transferable to the aforementioned anomalies (particle contamination and lubrication outage). The so-called center of energy γ indicates the time that elapses until half of the initial excitation energy from the sender has reached the receiver probe.

$$\gamma = \frac{1}{M}\sum_{i=1}^{n} n \cdot x_i \tag{3}$$

with M being the total energy of the signal in one excitation cycle. It has already been shown that the center of energy correlates with the friction intensity in a journal bearing. More explanations about the applied method can be found in [15].

3.2 Experimental setup

The experimental setup, including the journal bearing test rig and the lubrication circuit built for this work to induce the operational anomalies is shown in Fig. 4.

For the experiments the sliding speed v and the specific pressure $\overline{p}$ as well as the bearing temperature T can be controlled individually. The specific pressure $\overline{p}$ is applied via a hydraulic cylinder and the sliding speed v is set by the motor. The friction moment M_{Fr} can be determined using a friction gauge. The journal bearings tested have a diameter of $D = 120\,\text{mm}$ and a width of $B = 30\,\text{mm}$. The parameters of the test rig and the journal bearings are shown in Table 1. The test specimens are made of bronze and have no additional coating.

During the experiments the lubrication outage can be simulated by intentionally turning off the oil supply pump. The oil flow rate Q is measured by the volume flow sensor (cf. Fig. 4). Hereby, the lubrication outage can be detected. The particle contamination is induced by switching the three-way valve so that the whole oil flow is conducted through the bypass. The bypass has a built-in secondary

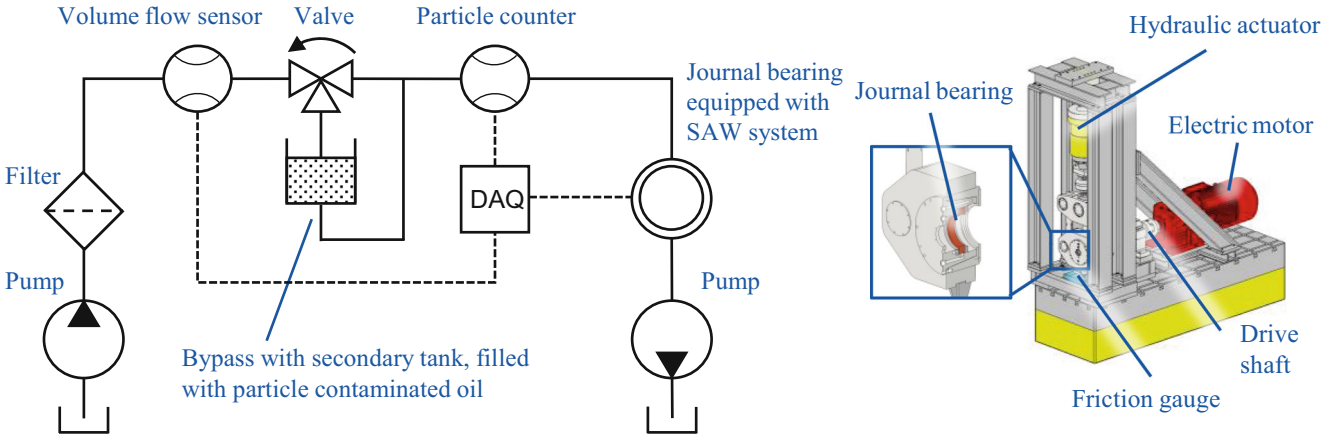

Fig. 4 Schematic depiction of the oil circuit (**a**) and the journal bearing test rig (**b**). (*DAQ* Data aquistion)

Table 1 Parameters of the test rig and the journal bearing

Test rig parameters	*Symbol/Unit*	*Value*
Radial force	F_R [kN]	0–216
Equals specific pressure	$\overline{p}$ [MPa]	0–60
Speed	n [1/ min]	0–580
Equals sliding speed	v [m/ sec]	0–3.6
Bearing temperature	T [°C]	20–100
Lubricant	[–]	ISO VG 320 (PAO)
Nominal bearing clearance	S [µm]	80
Journal bearing parameters		
Diameter	D [mm]	120
Width	B [mm]	30
Journal bearing material	–	CuSn12Ni2-C
Shaft material	–	42CrMo4
Young's modulus of journal bearing material	E_j [MPa]	100
Young's modulus of shaft material	E_s [MPa]	210

tank which is filled with particle contaminated oil. The secondary tank is filled with a defined amount of oil with a defined contamination according to ISO 4406 before the test procedure starts. During testing the oil from the tank will be flushed into the circuit as soon as the three-way valve gets switched. This method allows to induce the particle contamination at a dedicated time. Before the particles reach the journal bearing they pass a particle counter close to the bearing enclosure. This way the time of the particle contamination can be determined with sufficient precision. A laser-optical sensor was used for particle counting, which measures the concentration of particles in the lubricant in accordance with ISO 4406. According to the measurements in this work a reproducible amount of contamination can be flushed into the test bearing using the setup from Fig. 4.

3.3 Anomaly detection algorithm

In this work an anomaly detection method is used based on the method presented in [21]. The anomaly detection is based on a 2D-convolutional autoencoder as shown in Fig. 6. Convolutional autoencoders outperform classic neural networks in detecting anomalies in classical machine learning applications [21]. König et al. have shown that an anomaly detection based on an autoencoder and AE-measurements is possible for journal bearings [9]. The architecture of the autoencoder used in this work consists of an input and an output layer as well as three convolutional layers in between (cf. Fig. 5). The input data of the autoencoder consists of time sequences with n data points of the signal features center of energy γ, amplitude A and propagation time τ. Unlike a conventional neural network with fully connected layers of individual neurons, convolutional networks use filters which convolve over the input data in a specific stride. These filters can be used to compress

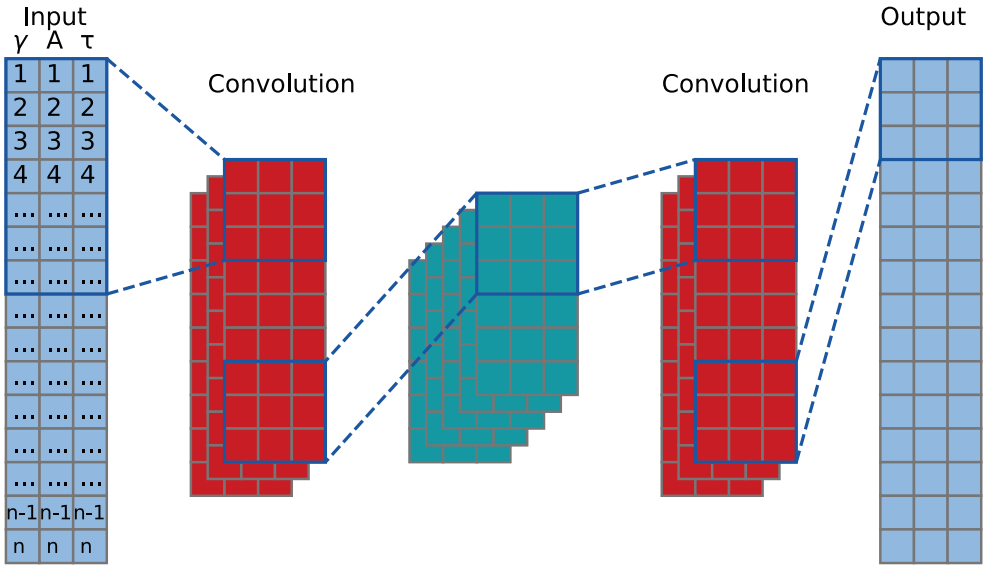

Fig. 5 Schematic presentation of the architecture of an 2D-convolutional autoencoder

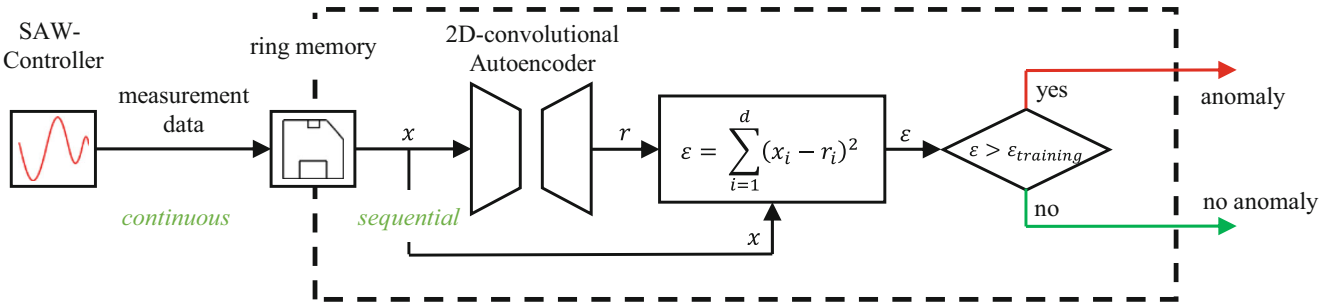

Fig. 6 Functionality of the anomaly detection algorithm

the information while emphasizing valuable patterns in the data. An autoencoder is divided into an encoder, a decoder and a bottleneck. The layers of the encoder contain a decreasing number of neurons with each layer. This leads to a compression of the input data that goes along with a loss of information.

The smallest layer of the autoencoder is called the bottleneck. Inside of the bottleneck the input data is compressed to its most salient features. After the compression the decoder recreates the input data based on the training information. The decoder usually has a mirrored architecture of the encoder. Due to the loss of information during the compression the recreation is always faulty to a certain quantifiable extend. The reconstruction loss ε can be calculated by Eq. 4.

$$\varepsilon = \sum_{i=1}^{d} (x_i - r_i)^2 \tag{4}$$

x_i represents the i-th component of the sequence x of the measurement data and r_i is analog i-th component of the reconstructed data.

Before the algorithm can be used for anomaly detection the autoencoder has to be trained. In the training phase the journal bearing is running in a hydrodynamic operating state. During this phase the SAW-controller transmits the data of the three signal features center of energy γ, amplitude A and propagation time τ continuously. The data gets saved in a ring memory. From this memory the data is transmitted to the autoencoder (cf. Fig. 6). During the training phase the autoencoder gets adjusted to minimize the reconstruction loss ε. After the training is completed the autoencoder can be used in the algorithm for anomaly detection [21]. The transmission of the measurement data is the same as during the training phase. For every sequence x of the measurement data the reconstruction loss ε is calculated using Eq. 4. Afterwards the reconstruction loss ε is compared to a threshold Θ. In this work the threshold Θ is the reconstruction loss $\varepsilon_{training}$ of the last training iteration. In case of an anomaly the measurement data deviates from the training data and the reconstruction loss ε exceeds the threshold $\Theta = \varepsilon_{training}$ [21]. In such a case the whole sequence is automatically labelled as an anomaly. For analysis

purposes the anomaly density ϱ_A is suitable. The anomaly density $\varrho_A$is calculated by:

$$\rho_A = \frac{n_{Anomaly}}{n_X} \in [0\%, 100\%] \tag{5}$$

ϱ_A is defined as the percentage ratio within one second sequences that are recognized as an anomaly $n_{Anomaly}$ and the number of all sequences examined during this period n_X. Analysis of the anomaly density allows for a qualitative evaluation of the anomaly labels over time.

4 Results

The experiments are separated in two groups: particle contamination and lubrication outage tests. Both test groups are performed following similar procedures. At first the bearing is operated in a hydrodynamic state for 600 sec. to create a reference measurement for the nominal operating condition. At $t = 600$ sec . the anomaly in the operation is created by flushing contaminated lubricant into the bearing (particle contamination experiment) or turning of the oil supply (lubrication outage experiment) according to Fig. 4a. The experiments are executed with a preconditioned specimen (run in bearing). The results are presented in the following.

4.1 Particle contamination experiments

In this section results of two particle contamination experiments are presented. The first experiment is carried out at a hydrodynamic operation point. The test parameters are shown in Table 2. The concentration of the iron particles in this experiment was determined through the analysis of oil samples taken from WT gearboxes in the field. After $t = 600\,sec$ the particles are injected into the oil stream and are flushed into the load zone of the bearing. An elasto-hydrodynamic simulation of the operating point tested here resulted in a minimum lubrication gap height of 1 µm. The particle contamination class used for this test includes particles that are larger than the minimum lubrication gap. It is assumed that three-body abrasion occurs in this condition, which is to be regarded as a critical condition for the journal bearing.

The measurement data of the particle contamination experiment is shown in Fig. 7. The graph of the friction moment M_{Fr} shows a negligible friction moment during the first 600 s of the experiment. At about $t = 650\,s$ the plot of the friction moment M_{Fr} shows a steep increase from about 2 Nm to over 22 Nm. This is an indicator for mixed friction that is induced by the injected particles. The oil flow Q is constant over the whole testing time and the bearing temperature T shows only a marginal increase at the peak of the friction moment M_{Fr}.

The propagation time τ and the propagation time modulation $\Delta\tau$ show an increase as soon as the particles reach the load zone of the bearing. The relative increase in the propagation time is 0.1 % and the signal behavior changes with the particle induction as the propagation time modulation $\Delta\tau$ shows. The change in acoustic propagation of SAW is also visible in the center of energy γ and amplitude A. The presence of particles in the lubrication gap and the mixed friction could lead to an increase in coupled out energy so that a reduction in the center of energy γ and the amplitude A gets visible. The fourth plot in Fig. 7 shows the anomaly density ϱ_A and the third number of the ISO 4406 contamination class which represents the particles larger than 14 µm. It is evident that the anomaly density ϱ_A is the highest at the peak of the friction moment M_{Fr}. The increase and the decrease of the anomaly density ϱ_A are similar to the friction moment M_{Fr}. This allows the conclusion that the autoencoder is able to detect the anomalies in good agreement with the friction occurring in the bearing. The 14 µm-signal of the particle counter (ISO 4406: 14 µm in Fig. 7) installed in the oil supply of the test rig (cf. Fig. 4) is in good agreement with the signal pattern of the friction moment M_{Fr} and the anomaly density ϱ_A, which further validates the results. Figure 8 shows a microscopic image taken from the sliding surface within the load zone of the specimen used for the first particle contamination experiment. The bearing load zone shows scoring caused by abrasive wear (three-body-abrasion). Embedded particles can be seen in one of the grooves material analysis using the electron microscope revealed that the embedded particle marked in Fig. 8 is an iron particle. In summary, the experiment with a particle

Table 2 Test parameters of the first particle contamination experiment

Parameter	Symbol/Unit	Value
Specific pressure	$\overline{p}$[MPa]	10
Sliding speed	v[m/ sec]	0.1
Test duration	t_{total}[sec]	1800
Time of anomaly	$t_{anomaly}$[sec]	600
Particle material	[–]	Iron
Contamination class during anomaly (ISO 4406)	[–]	20/19/13
Particle concentration	c[g/100g]	0.1

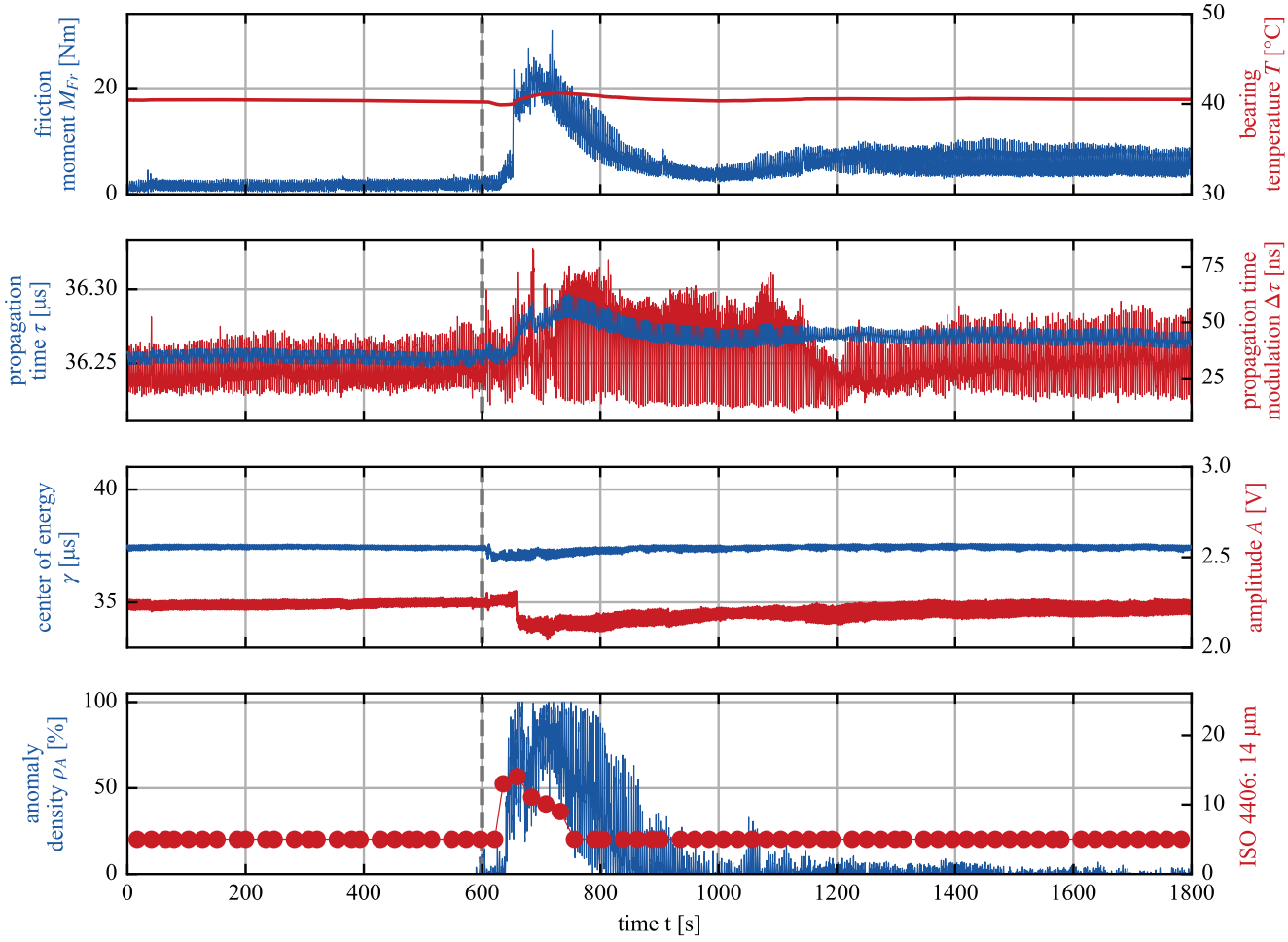

Fig. 7 Measurement data of the first particle contamination experiment. Including the test rig data, SAW-data and the detected anomalies

concentration of 0.1 $g/100\,g$ lled to satisfactory results in terms of detectability of the anomaly. However, the particle injection in the experiment caused significant abrasion on the bearing's sliding surface. Therefore, the detection of a significantly lower particle concentration than in the first experiment appears desirable. In a second experiment a lower particle concentration c (0.01 $g/100\,g$) is investigated (see also Fig. 9).

The concentration c used in this second experiments leads to a ISO 4406 contamination class measured of 20/19/7 (for comparison: the ISO 4406 class of the other experiment is 20/19/13). The other experimental parameters were kept equal to the aforementioned experiment (see Table 2). At $t = 600\,s$ the particles were induced into the oil stream. 40 s later the particles reach the lubrication gap of the bearing as the contamination level in Fig. 9 indicates and the friction moment increases slightly from about 2 Nm to around 4.3 Nm. Furthermore, a small increase in propagation time modulation $\Delta\tau$ is detected at this time. In comparison to the measurements in Fig. 7 the increase in contamination, friction moment M_{Fr} and propagation time modulation $\Delta\tau$ is much smaller. Nevertheless, the anomaly density ϱ_A also peaks two times although smaller as in the previous contamination experiment. The first peak is caused by a pressure surge due to switching to the bypass. The second peak is in good alignment with the 14 µm-signal of the particle counter and correlates with the friction moment M_{Fr} as well. This leads to the assumption that the anomaly detection method is working for low contamination levels as well and that the percentage of labeled anomalies A correlates with the criticality of the anomaly.

4.2 Lubrication outage experiment

Additionally, to the particle contamination experiment, a lubrication outage experiment is shown in this section. The operating parameters of this experiment are listed in Table 3.

The results of the lubrication outage experiment are presented in Fig. 10. Analogous to the particle contamination experiment, the bearing is running in a hydrodynamic operating point as the experiments starts. At $t_{Anomaly}$ = 600 sec

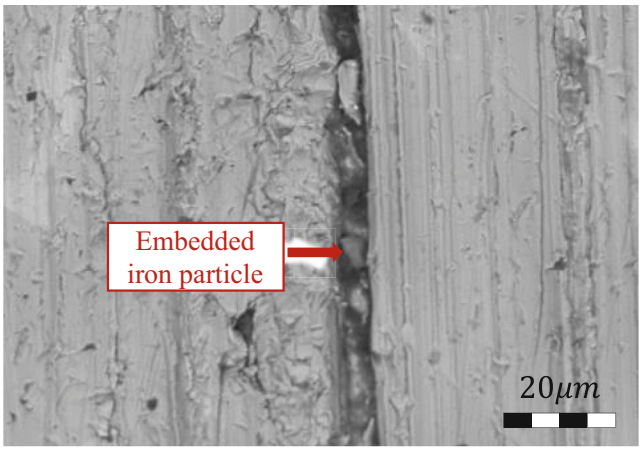

Fig. 8 High resolution image of the bearing sliding surface in the load zone captured by an electron microscope

the oil pump is turned off and the oil flow Q decreases to 0l/min instantly. After 200 s at t = 800 sec the friction moment M_{Fr} increases slowly. This shows that the oil is flushed from the load zone and the bearing starts to operate in mixed friction. At this time the temperature T starts to increase slowly.

The maximum increase from t = 800 sec to t = 1200 s is ΔT = 2°C which can be seen as neglectable. At t = 1200 sec the oil pump is turned on and the oil flow rises to Q = 8.5l/ min again. Immediately after the oil pump is turned on again, the friction moment M_{Fr} decreases to the starting value of 3 Nm. This shows that the bearing is running in hydrodynamic operation again. In Fig. 10 the SAW-features propagation time τ and the propagation time modulation $\Delta\tau$ are shown analog to the particle contamination experiments. During the anomaly the propagation time τ increases by about 0.02—s, which is a small change in comparison to the particle contamination experiment. Increased amplitude modulation can be seen in the propagation time signal between $t_{Anomaly}$ = 600 secand t = 1200 sec. The propagation time modulation $\Delta\tau$ increases from < 5ns to 50ns at $t_{Anomaly}$ = 600 sec. The output signal from the autoencoder is shown in Fig. 9, filtered in the same way as in Fig. 7. The autoencoder detects many anomalies right after $t_{Anomaly}$ = 600 sec. This is analogous to the high propagation

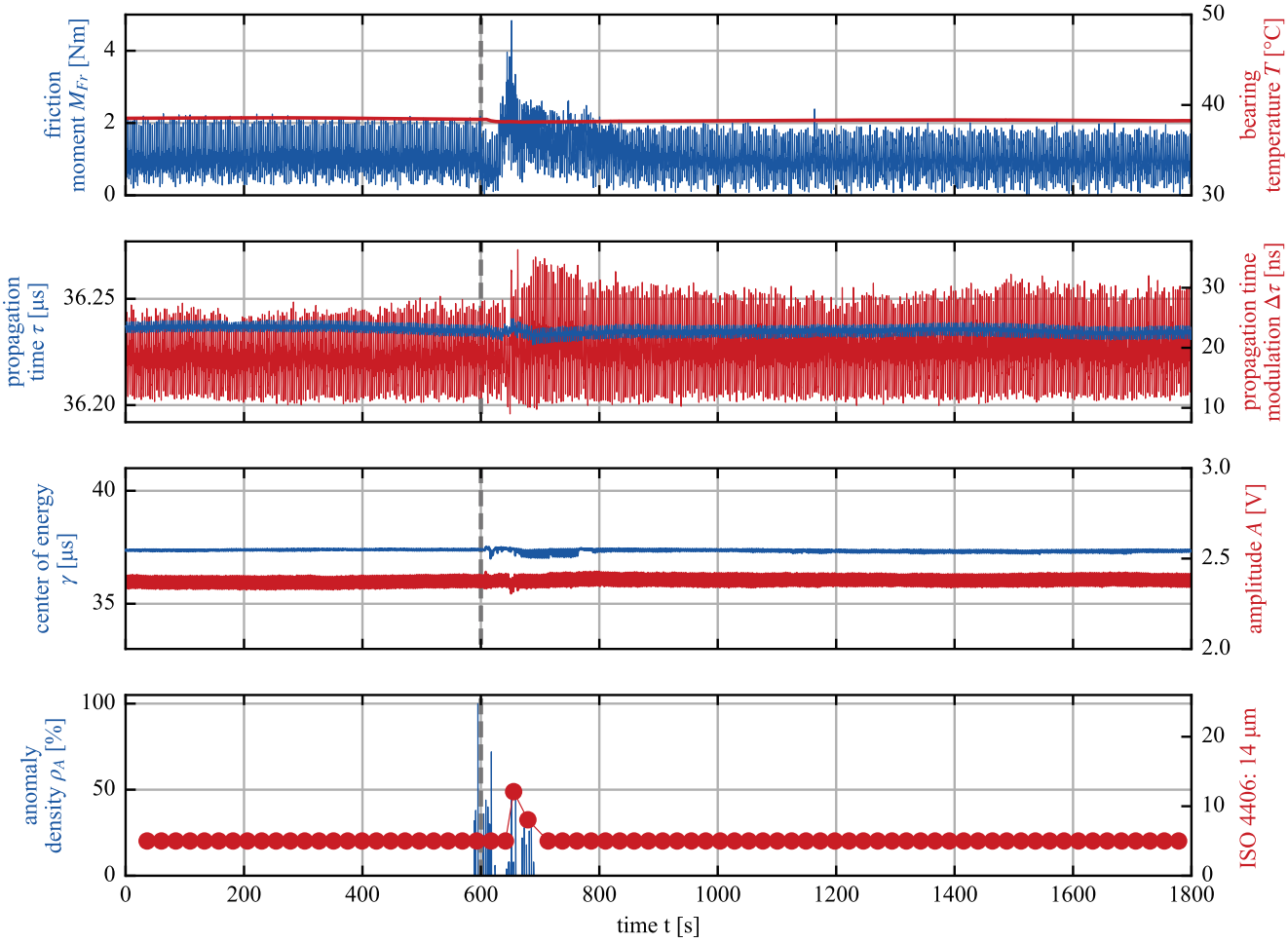

Fig. 9 Measurement data of the second particle contamination experiment. Including the test rig data, SAW-data and the detected anomalies

Table 3 Test parameters of the lubrication outage tests

Parameter	Symbol/Unit	Value
Specific pressure	$\overline{p}$[MPa]	20
Sliding speed	v[m/s]	0.4
Test duration	t_{total}	30
Time of anomaly	$t_{anomaly}$	10

time modulation $\Delta\tau$. At $t = 800$ sec the number of detected anomalies A starts to increase parallel to the increase of the friction moment M_{Fr}. This observation corresponds to the results of the particle contamination experiment where a correlation between the detected anomalies A and the friction moment M_{Fr} can be observed. The great advantage of the SAW method over conventional condition monitoring metrics for journal bearings is evident here: an increase in the frictional moment M_{Fr} is immediately visible through the acoustic modulation of the SAW. It can be expected that a qualitative estimation of the frictional moment is also possible under real conditions in the field, since the friction moment correlates with the propagation time modulation of the SAW.

For a second lubrication outage experiment the operating point is nearly the same as in Table 3, except the specific pressure $\overline{p}$ is at 10 MPa. The results are presented in Fig. 11. As with all the experiments shown above, the autoencoder was trained with the initial, hydrodynamic operating point for each test. The measurement data shows the highest increase in friction moment M_{Fr}, bearing temperature T, propagation time τ and propagation time modulation $\Delta\tau$. The increase in propagation time modulation $\Delta\tau$ is so large that it is shown in logarithmic scale. In contrast to the previous experiment, the oil supply is turned on again at $t = 950$ sec because a longer lubrication outage would most likely have ended in a bearing failure.

These results show how damaging the operational anomalies are: the lubrication outage leads to wear that changed the acoustic behavior of the bearing surface. This can be observed looking at the center of energy γ and the amplitude A which have different values before and after the anomaly (amplitude A: 4.2 V before and 3.8 V afterwards). If the

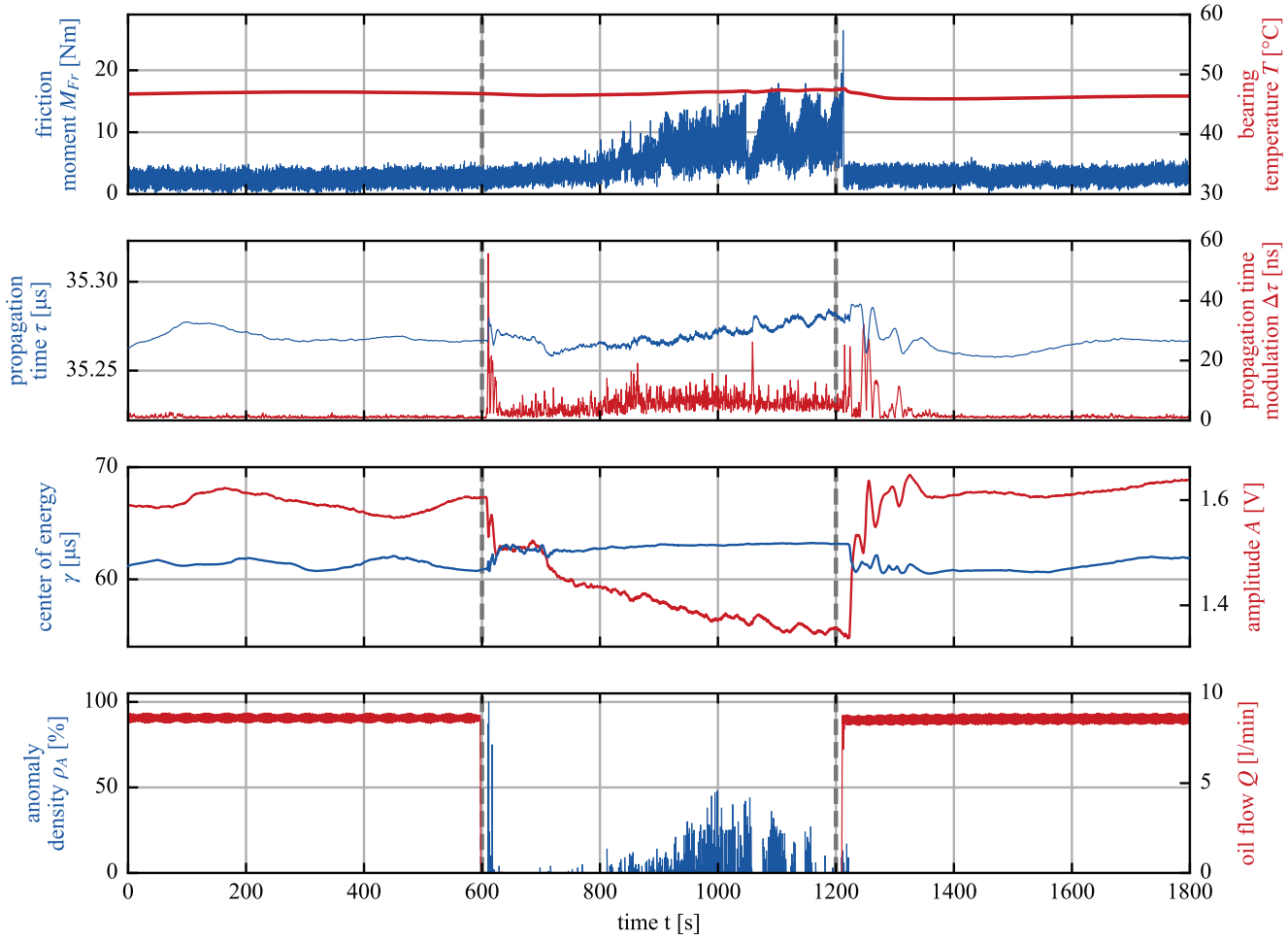

Fig. 10 Measurement data of the lubrication outage experiment. Including the test rig data, SAW-data and the detected anomalies

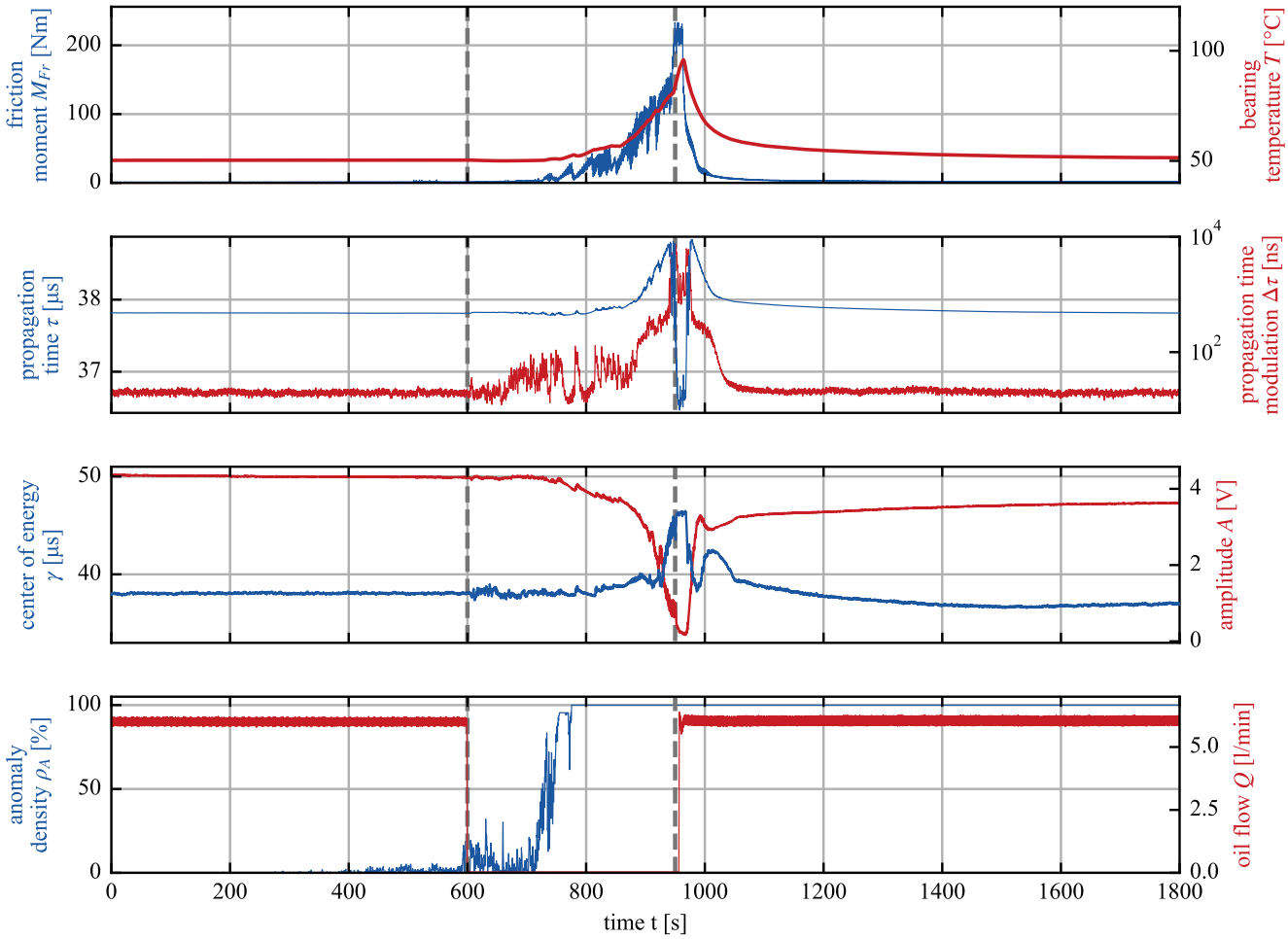

Fig. 11 Measurement data of the critical lubrication outage experiment. Including the test rig data, SAW-data and the detected anomalies

bearing is pre-damaged (in this case due to the experiment presented in Fig. 10) the emergency running properties are worsening so that in this case a second anomaly with only half the specific pressure $\overline{p}$ is enough to cause lasting damage on the bearing.

5 Conclusion

This paper presents a method to detect particle contamination and a shortfall of lubrication in journal bearings using SAW-measurements. The results show that the SAW method has the potential to detect the anomalies with a short latency. In all experiments a strong increase in the propagation time modulation $\Delta\tau$ is detected after the beginning of the anomaly. A high propagation time modulation $\Delta\tau$ is caused by the discontinuous and statistically distributed asperity contacts, as this causes noise in the propagation time τ signal. In this work the SAW measurements are analyzed using an anomaly detection algorithm based on an autoencoder. The number of detected anomalies over time is expressed through the so-called anomaly density ϱ_A. The results for ϱ_A are consistent with the particle contamination and lubrication outage during the experiments, but also respond to other changes in operating conditions. It can be concluded that the though the SAW method is characterized by its strong robustness against acoustic disturbances, the evaluation of this measurement poses a particular challenge in terms of the robustness of the diagnostic algorithm used.

The notable advantage of the presented method lies in the correlation of the SAW propagation time modulation $\Delta\tau$ of with the friction moment. In the experimental environment (test rigs) the resulting frictional moment can be measured easily and precisely. In the field application, where the CMS is to be used, this measurement is typically not available. The high sensitivity and the short latency make the method suitable for the condition monitoring task of journal bearings. Furthermore, the ability to manually set the excitation frequency makes the SAW-system resistant against interferences. The disadvantage of the system is a high construction and assembly effort. The probes must be placed in the bearing which demands a method to in-

clude the sensors and the controllers into a rotating part of the gearbox.

6 Outlook

The results presented show that the combination of the SAW system with a machine learning algorithm is suitable for detecting anomalies in journal bearings. However, the method of this work needs to be improved in order to work as a condition monitoring system. In the experiments presented, the training of the autoencoder took place just before the start of the experiment. This means that the autoencoder is trained for only one hydrodynamic operation point and any change (e.g. a different fluid film height) could be detected as an anomaly. One focus of the next steps is therefore to develop an autoencoder that is trained in different operating states. Another focus is the classification of the anomaly. Research has shown that machine learning algorithms are able to distinguish between lubrication failure, particle contamination and mixed friction [16, 17]. These works were performed using AE signals. AE is susceptible to interferences and comes with very large data. SAW is less prone to disturbances and the measurement data is smaller.

Secondly, the present study is limited to component level experiments. Future work will aim to demonstrate the applicability of the SAW method to a WT gearbox system where the SAW method will be used to monitor the operating condition of planetary journal bearings.

Acknowledgements The authors would like to thank the Ministry of Economic Affairs and Climate Action of Germany, for the financial support granted. They also thank their project partners for the equipment, insight as well as expertise they have provided, which contributed to this joint project.

Supported by:

Federal Ministry
for Economic Affairs
and Climate Action

on the basis of a decision
by the German Bundestag

Funding Open Access funding enabled and organized by Projekt DEAL.

Conflict of interest T. Decker, G. Jacobs, M. Raddatz, J. Röder, J. Betscher and P. Arneth declare that they have no competing interests.

References

1. Umweltbundesamt (2024) Erneuerbare Energien in Deutschland: Daten zur Entwicklung im Jahr
2. Statistisches Bundesamt (2024) Bruttostromerzeugung 2023. https://www.destatis.de/DE/Themen/Branchen-Unternehmen/Energie/_Grafik/_Interaktiv/bruttostromerzeugung-erneuerbare-energien.html. Accessed 23 Mar 2024
3. Thys T, Smet W (2023) Selective assembly of planetary gear stages to improve load sharing. Forsch Ingenieurwes 87:275–283. https://doi.org/10.1007/s10010-023-00646-x
4. Marheineke J (2024) Ermittlung und Bewertung des Verhaltens von hydrodynamischen Gleitlagern bei Mangelschmierung. Dissertation, RWTH Aachen University
5. Boucherit H, Bou-Saïd B, Lahmar M (2017) The effect solid particle lubricant contamination on the dynamic behavior of compliant journal bearings. Lubr Sci 29:425–439. https://doi.org/10.1002/ls.1378
6. Marheineke J, Jacobs G (2023) Betriebspunktabhängige Qualifizierung und Auswahl von Gleitlagerwerkstoffen (Werkstoffqualifizierung)
7. Poddar S, Tandon N (2019) Detection of particle contamination in journal bearing using acoustic emission and vibration monitoring techniques. Tribol Int 134:154–164. https://doi.org/10.1016/j.triboint.2019.01.050
8. Poddar S, Tandon N (2020) Study of Oil Starvation in Journal Bearing Using Acoustic Emission and Vibration Measurement Techniques. J Tribol. https://doi.org/10.1115/1.4047455
9. König F, Jacobs G, Stratmann A et al (2021) Fault detection for sliding bearings using acoustic emission signals and machine learning methods. IOP Conf Ser. Mater Sci Eng 1097:12013. https://doi.org/10.1088/1757-899X/1097/1/012013
10. Baszenski T, Kauth K, Kratz K-H et al (2023) Sensor integrating plain bearings: design of an energy-autonomous, temperature-based condition monitoring system. Forsch Ingenieurwes 87:441–452. https://doi.org/10.1007/s10010-023-00642-1
11. Yu L, Giurgiutiu V (2012) Piezoelectric Wafer Active Sensors in Lamb Wave-Based Structural Health Monitoring. JOM 64:814–822. https://doi.org/10.1007/s11837-012-0362-9
12. Lindner G, Schmitt M, Schubert J et al (2010) On-line surveillance of lubricants in bearings by means of surface acoustic waves. IEEE Trans Ultrason Ferroelectr Freq Control 57:126–132. https://doi.org/10.1109/TUFFC.2010.1388
13. Lindner G, Brückner C, Schmitt M (2011) Online Bearing Lubricant Sensing by Mode Conversion of Surface Acoustic Waves
14. Rose JL (2014) Ultrasonic Guided Waves in Solid Media. Cambridge University Press
15. Decker T, Jacobs G, Arneth P et al (2024) Approach towards the condition monitoring of journal bearings using surface acoustic wave technology. Bear World J 8

16. König F, Sous C, Ouald Chaib A et al (2021) Machine learning based anomaly detection and classification of acoustic emission events for wear monitoring in sliding bearing systems. Tribol Int 155:106811. https://doi.org/10.1016/j.triboint.2020.106811
17. Poddar S, Tandon N (2021) Classification and detection of cavitation, particle contamination and oil starvation in journal bearing through machine learning approach using acoustic emission signals. Proc Inst Mech Eng Part J: J Eng Tribol 235:2137–2143. https://doi.org/10.1177/1350650121991316
18. Tchakoua P, Wamkeue R, Ouhrouche M et al (2014) Wind Turbine Condition Monitoring: State-of-the-Art Review, New Trends, and Future Challenges. Energies 7:2595–2630. https://doi.org/10.3390/en7042595
19. BestSens AG (2021) Handbuch zum BeMoS® One IEPE
20. Tyreas G, Dwyer-Joyce RS, Notay RS et al (2022) Measuring lubricant viscosity at a surface and in a bearing film using shear-horizontal surface acoustic waves. Proc Inst Mech Eng Part J: J Eng Tribol 236:1511–1530. https://doi.org/10.1177/13506501221092867
21. Chen Z, Yeo CK, Lee BS et al (2018) Autoencoder-based network anomaly detection. In: 2018 Wireless Telecommunications Symposium (WTS). IEEE, pp 1–5